Available online at www.sciencedirect.com
SCIENCE DIRECT®
Journal of Sound and Vibration 291 (2006) 824–843
JOURNAL OF SOUND AND VIBRATION
www.elsevier.com/locate/jsvi

Iterative solution of high-order boundary element method for acoustic impedance boundary value problems

P. Ylä-Oijala*, S. Järvenpää

Electromagnetics Laboratory, Helsinki University of Technology, P.O. Box 3000, FIN-02015 HUT, Finland

Received 9 February 2004; received in revised form 26 May 2005; accepted 28 June 2005
Available online 4 January 2006

Abstract

A high-order boundary element method for time-harmonic acoustic impedance boundary value problems is presented. The method is based on the Galerkin-type formulation of the Burton–Miller integral equation (BMIE) with high-order polynomial basis and testing functions. This formulation has several important advantages: It is free of the interior resonance problem, the hypersingular integral operator of the traditional BMIE formulation can be avoided, it leads to faster convergence in terms of the number of unknowns than the low-order methods and it shows a good performance with iterative solvers. To avoid the numerical difficulties associated to the implementation of the singular surface integral equations, the singularity extraction technique is applied to evaluate the integrals in the singular and near-singular cases. The resulting matrix equation is solved iteratively with the generalized minimal residual method (GMRES) and a simple preconditioner based on the incomplete LU factorization is applied to expedite the convergence. Numerical results indicate that the BMIE formulation with Galerkin method and high-order basis functions has good convergence properties for various geometries and boundary conditions on a wide frequency range when the GMRES method is applied to solve the matrix equation iteratively. This, in turn, indicates that the formulation is well suited for an efficient application of fast solution procedures, such as the fast multipole method.

1. Introduction

Integral equation methods have been widely used to solve various time harmonic acoustic problems. For open-region problems the boundary element method (BEM) is attractive since the radiation conditions are automatically satisfied and the dimensionality of the problem is decreased by one. One drawback of the BEM is that for the exterior acoustic problems the traditional integral equation formulations suffer from the problem of interior resonances [1]. These frequencies are due only to the numerical method, which has no unique solution at some eigenfrequencies of the corresponding interior problem. Two methods have been proposed to remove this non-uniqueness problem. In the first method, the Combined Helmholtz Integral Equation Formulation (CHIEF) [2,3], a set of interior collocation points are taken as an auxiliary condition to overdetermine the equations and to make up a deficient condition. However, the number and position of the

*Corresponding author. Fax: +358 9 451 2267.
E-mail addresses: pasi.yla-oijala@hut.fi (P. Ylä-Oijala), seppo.jarvenpaa@hut.fi (S. Järvenpää).

0022-460X/$ - see front matter © 2005 Elsevier Ltd. All rights reserved.
doi:10.1016/j.jsv.2005.06.044

points are usually case dependent and difficult to determine for complicated structures [4,5]. In the second method, Burton–Miller integral equation (BMIE) formulation (also known as Composite Outward Normal Derivative Overlap Relation (CONDOR)) [6], a linear combination of the Kirchhoff–Helmholtz integral equation and its normal derivative is applied. The drawback of the BMIE is that it includes a hypersingular integral operator and special techniques are required to regularize it [7–11]. In Refs. [12–15], Demkowicz and Oden et al. presented an alternative weakly singular formulation of the BMIE, which is solved with the Galerkin method and the derivatives of the hypersingular integral operator are transformed from the singular kernel into non-singular testing and basis functions. The resulting weak form includes only weakly singular integral operators and complicated regularization schemes can be avoided.

The BEM has two major numerical difficulties. Firstly, the integral kernels are singular as the field point coincides with the source point. Traditional integration schemes like a Gaussian quadrature usually gives results that are too inaccurate, leading to ineffective and slowly converging solution. Integration of singular terms has been considered in the literature by both numerical and (semi-)analytical techniques. Widely applied numerical techniques are for example Duffy's method [16] and polar coordinate transformation [17]. Another approach that can be applied on planar triangular elements is to use the singularity extraction technique [18,19]. In this method a suitable singular term is extracted from the kernel and integrated analytically.

The second drawback of the BEM is that discretization of an integral equation leads to a dense system matrix which is expensive to store and solve. A direct solution of such linear system requires $\mathcal{O}(N^3)$ CPU time and $\mathcal{O}(N^2)$ computer memory, where N is the number of unknowns. These numbers are prohibitively expensive for large-scale three-dimensional problems. There are several strategies available for high-wavenumber problems. One possibility is to increase the order of the approximation of the unknown function. In Refs. [13,14], Demkowicz et al. apply adaptive high-order methods in elastic and acoustic scattering problems. In Ref. [20] Gennaretti et al. use third-order basis functions and point collocation to solve the BMIE. In Ref. [21] Harris and Chen apply piecewise polynomial basis functions and Galerkin method for acoustic scattering by rigid objects. With the high-order basis functions higher accuracy can be obtained with a reduced number of unknowns [21], but the CPU time and memory requirements are still the same as with the low-order methods.

Another possibility to reduce the computational cost is to solve the matrix equation with iterative methods, such as the conjugate gradient method [22] or the generalized minimal residual method (GMRES) [23]. Iterative methods typically reduce the CPU time requirement to $N_{\text{iter}}\mathcal{O}(N^2)$, where N_{iter} is the number of iterations in which convergence is achieved. In Ref. [24] Amini and Maines apply these Krylov subspace methods to solve BMIE in two dimensions. In Ref. [25] Chen and Harris study iterative solution of the BMIE in three dimensions when the point collocation technique was applied to discretize the integral equation. Later in Ref. [21] the same authors consider iterative solution of the high-order Galerkin discretization of the BMIE formulation. In Refs. [26,27], Marburg and Schneider compare four different iterative methods for solving BMIE with discontinuous basis functions. In Ref. [28], the authors apply an improved GMRES method for solving acoustic scattering problems. However, in some cases iterative solvers may converge rather slowly leading to a long computing time. A usual technique to expedite the convergence of an iterative solver is preconditioning [29,30]. In the aforementioned papers several techniques were investigated, including, e.g. periodic triangular preconditioner [24], one based on operator splitting [25,21], diagonal [26] and incomplete LU factorization [27].

The CPU time and memory requirements of an iterative solver are, although convergence is achieved in a relative low number of iterations, still fairly high for dense matrix equations making them impractical for problems with a very high number of unknowns and additional techniques, so-called fast methods, are required to further reduce the computational cost. Widely applied fast methods based on speeding up the calculation of the matrix–vector product of an iterative solver are, e.g. the fast multipole method (FMM) [31], its multilevel version, multilevel fast multipole algorithm (MLFMA) [32], and the fast Fourier transform-(FFT) based methods [33,34]. Recent applications of these methods in computational acoustics can be found, e.g. in Refs. [35–38]. Other approaches to consider high-wavenumber problems, including microlocal discretization [39] and plane wave basis BEM [40], are presented in Ref. [41] and references therein.

In this paper, some of the aforementioned difficulties of the BEM are addressed in the context of time-harmonic acoustic impedance boundary value problems. The implementation is based on the Galerkin-type discretization of the BMIE formulation. The weakly singular weak form of BMIE formulation of Ref. [12] is

solved with the high-order polynomial basis and testing functions. To avoid numerical difficulties associated to the implementation of the singular surface integral equations, the singularity extraction technique is applied to evaluate the integrals of the BMIE formulation in the singular and near-singular cases. Recently, this method has been generalized for the high-order integral equation methods in Ref. [42] and applied for solving electrostatic field problems with the high-order basis functions in Ref. [43].

In order to consider problems with a higher number of unknowns, iterative solution of a dense linear system arising from the high-order Galerkin discretization of the BMIE formulation is studied with the GMRES method. To expedite the convergence of the GMRES method a simple incomplete LU preconditioner [44] is developed. Similar preconditioning technique has been applied successfully in the electromagnetic scattering problems in Refs. [45,46] and also in the acoustic scattering problems [27]. One of the main objectives of this paper is to demonstrate that the high-order BEM based on the BMIE formulation and discretized via the Galerkin method is well-conditioned for various boundary conditions and geometries on a wide frequency range. As a result, the developed formulation leads to rapidly converging iterative solutions and is a very promising candidate for an efficient application of fast methods, like the MLFMA.

2. Statement of the problem

Consider scattering of time-harmonic acoustic waves by a bounded impenetrable object D in a homogeneous medium in three dimensions. The time factor is $e^{-i\omega t}$ with the frequency $\omega = 2\pi f$. Let $k_0 = \omega/c_0$ denote the wavenumber of the homogeneous background, where c_0 is the speed of sound. Let the object D be impinged with an incident acoustic wave, let p^{inc} denote the pressure of the incident wave and let p^{sca} denote the pressure of the scattered wave. In the sequel, the exterior of D is denoted by D^{ext} and the surface of D is denoted by S.

The task is to find p^{sca} so that it satisfies homogeneous Helmholtz equation outside D

$$(\nabla^2 + k_0^2)p^{\text{sca}}(\mathbf{r}) = 0, \quad \mathbf{r} \in D^{\text{ext}} \tag{1}$$

and the pressure of the total wave, $p = p^{\text{inc}} + p^{\text{sca}}$, satisfies the impedance boundary condition on the surface of D

$$\frac{\partial p}{\partial n}(\mathbf{r}) = \eta(\omega, \mathbf{r})p(\mathbf{r}) + g(\mathbf{r}), \quad \mathbf{r} \in S. \tag{2}$$

Here $\eta(\omega, \mathbf{r}) = -i\omega\rho\, Y(\mathbf{r})$, ρ is the density, Y is a complex-valued surface admittance with the positive real part and g is a given function. In addition, the scattered pressure must satisfy the Sommerfeld radiation condition at infinity [1]

$$\lim_{r\to\infty} r\left|\frac{\partial p^{\text{sca}}}{\partial r} - ik_0 p^{\text{sca}}\right| = 0, \tag{3}$$

where $r = |\mathbf{r}|$. This exterior boundary value problem has a unique solution for all k_0 provided that $\text{Im}(\eta) \leqslant 0$ [1].

3. Boundary element method

In this section, we introduce the BEM in solving the aforementioned exterior boundary value problem of the Helmholtz equation.

3.1. Integral equations

Let us begin by defining the following four integral operators at points $\mathbf{r} \in D^{\text{ext}}$

$$(\mathcal{S}p)(\mathbf{r}) := \int_S G(\mathbf{r}, \mathbf{r}')p(\mathbf{r}')\, dS', \tag{4}$$

$$(\mathscr{K}p)(\mathbf{r}) \coloneqq \int_S \frac{\partial G}{\partial n'}(\mathbf{r},\mathbf{r}')p(\mathbf{r}')\,\mathrm{d}S', \tag{5}$$

$$(\mathscr{M}p)(\mathbf{r}) \coloneqq \int_S \frac{\partial G}{\partial n}(\mathbf{r},\mathbf{r}')p(\mathbf{r}')\,\mathrm{d}S', \tag{6}$$

$$(\mathscr{N}p)(\mathbf{r}) \coloneqq \frac{\partial}{\partial n}\int_S \frac{\partial G}{\partial n'}(\mathbf{r},\mathbf{r}')\,p(\mathbf{r}')\,\mathrm{d}S'. \tag{7}$$

Here

$$G(\mathbf{r},\mathbf{r}') = \frac{\mathrm{e}^{\mathrm{i}k_0|\mathbf{r}-\mathbf{r}'|}}{4\pi|\mathbf{r}-\mathbf{r}'|} \tag{8}$$

is the Green's function of the homogeneous background and $\partial/\partial n'$ and $\partial/\partial n$ denote normal derivatives with respect to the primed and unprimed coordinates, respectively, with the normal vectors pointing into the exterior.

The integral representation for the pressure of the sound wave scattered from the object D can be written in D^{ext} as [1]

$$p^{\mathrm{sca}}(\mathbf{r}) = (\mathscr{K}p)(\mathbf{r}) - \left(\mathscr{S}\frac{\partial p}{\partial n}\right)(\mathbf{r}), \quad \mathbf{r} \in D^{\mathrm{ext}}. \tag{9}$$

By letting $\mathbf{r} \to S$, denoting $p^{\mathrm{sca}} = p - p^{\mathrm{inc}}$, and by rearranging the terms, integral equation (9) on S takes the form [1]

$$\left(\mathscr{K} - \frac{1}{2}\mathscr{I}\right)(p)(\mathbf{r}) - \left(\mathscr{S}\frac{\partial p}{\partial n}\right)(\mathbf{r}) = -p^{\mathrm{inc}}(\mathbf{r}), \quad \mathbf{r} \in S. \tag{10}$$

Here $\mathscr{I}$ denotes the identity operator. Since this equation includes two unknowns, p and $\partial p/\partial n$, boundary condition (2) must be applied to have a relation for the unknowns and to eliminate one of them. Eq. (10) (with the boundary condition), however, does not give unique solution for all frequencies [1]. This non-uniqueness problem is known as the problem of interior resonances and it is a purely mathematical problem arising from the breakdown of the boundary integral formulation rather than from the nature of the physical problem. To avoid this, BMIE formulation [6] is applied instead of Eq. (10). BMIE is a linear combination of the Kirchhoff–Helmholtz integral equation (10) and its normal derivative with an appropriate coupling coefficient β. With the operator notations (4)–(7), the BMIE can be written at points $\mathbf{r} \in S$ as

$$\left(\mathscr{K} - \frac{1}{2}\mathscr{I}\right)(p) - \left(\mathscr{S}\frac{\partial p}{\partial n}\right) + \beta\left((\mathscr{N}p) - \left(\mathscr{M} + \frac{1}{2}\mathscr{I}\right)\left(\frac{\partial p}{\partial n}\right)\right) = -p^{\mathrm{inc}} - \beta\frac{\partial p^{\mathrm{inc}}}{\partial n}. \tag{11}$$

If the coupling coefficient β has a non-zero imaginary part, Eq. (11) with the boundary condition (2) has a unique solution for all real and positive k [6]. We choose the parameter β as [47,48]

$$\beta = \begin{cases} 2\mathrm{i}r, & k_0\, r \leqslant \dfrac{1}{2}, \\ \dfrac{\mathrm{i}}{k_0}, & k_0\, r > \dfrac{1}{2}, \end{cases} \tag{12}$$

where r is the radius of the smallest sphere enclosing the object D. This choice is nearly optimal for a sphere and it appears to be reasonable for other shapes too.

3.2. Galerkin method

One of the main difficulties in solving Eq. (11) numerically is the numerical calculation of the hypersingular integral operator $\mathscr{N}$. By moving the derivative with respect to the unprimed coordinate under the integral, we see that the kernel of $\mathscr{N}$ behaves as $\mathscr{O}(1/R^3)$, where $R = |\mathbf{r}-\mathbf{r}'|$ [15], and special regularization techniques are required to handle this operator [7–11]. These regularization techniques are usually based on the point

collocation method and on extracting sufficiently many terms from the Green's function and/or from the unknown function. In this paper, however, an alternative approach based on the Galerkin method is applied. Using Galerkin method the derivatives operating on the singular Green's function can be transferred into non-singular basis and testing functions and the resulting weak form of the BMIE includes only weakly singular integral operators [12–15]. This decreases the order of complexity of the method and makes numerical evaluation of the singular integrals clearly more straightforward and efficient, and no special regularization techniques are required. Usually Galerkin method is avoided because it requires integration over the surfaces twice and hence it is computationally more expensive than the point collocation method. On the other hand, numerical studies have indicated that the (high-order) Galerkin method leads to clearly faster solution convergence in terms of the number of unknowns than the (constant) point collocation method [21].

3.2.1. Weakly singular weak form of BMIE

Before applying Galerkin method to convert BMIE into a matrix equation, the weak form of Eq. (11) including only weakly singular integral operators is reviewed. On a closed and smooth surface S, operator $\mathcal{N}$ can be decomposed into two terms as [12,20]

$$(\mathcal{N}p)(\mathbf{r}) = \mathbf{n}\cdot\left(\nabla\times\int_S G(\mathbf{r},\mathbf{r}')\mathbf{rot}'\,p(\mathbf{r}')\,\mathrm{d}S'\right) + k_0^2\int_S \mathbf{n}\cdot\mathbf{n}'G(\mathbf{r},\mathbf{r}')p(\mathbf{r}')\,\mathrm{d}S', \tag{13}$$

where $\mathbf{r}\in S$ and

$$\mathbf{rot}'\,p = \mathbf{n}'\times\nabla' p. \tag{14}$$

Vectors $\mathbf{n}=\mathbf{n}(\mathbf{r})$ and $\mathbf{n}'=\mathbf{n}(\mathbf{r}')$ are the unit normals of S pointing into D^{ext}. Using Eq. (13) BMIE (11) can be rewritten as

$$\left(\mathcal{K}-\frac{1}{2}\mathcal{I}\right)(p) - \left(\mathcal{S}\frac{\partial p}{\partial n}\right) + \beta\big(\mathbf{n}\cdot\nabla\times\mathcal{S}(\mathbf{rot}'p) + k_0^2\mathcal{S}(\mathbf{n}\cdot\mathbf{n}'p) - \left(\mathcal{M}+\frac{1}{2}\mathcal{I}\right)\left(\frac{\partial p}{\partial n}\right)\Big) = -p^{\mathrm{inc}} - \beta\frac{\partial p^{\mathrm{inc}}}{\partial n}. \tag{15}$$

The next question is how to consider the curl operator in the third term on the left-hand side of Eq. (15). By using Galerkin method, i.e. by multiplying Eq. (15) with a (Hölder) continuous testing function v, integrating over the surface S and then using Stoke's theorem, the curl term can be written as [12]

$$\int_S v(\mathbf{r})\mathbf{n}\cdot(\nabla\times\mathcal{S}(\mathbf{rot}'p))\,\mathrm{d}S = -\int_S \mathbf{rot}\,v(\mathbf{r})\cdot\mathcal{S}(\mathbf{rot}'p)\,\mathrm{d}S, \tag{16}$$

where $\mathbf{rot}\,v=\mathbf{n}\times\nabla v$. The right-hand side of Eq. (16) includes only a weakly singular integral operator $\mathcal{S}$. Thus, by using Galerkin method and Eqs. (13) and (16), the hypersingular operator $\mathcal{N}$ can be replaced with two weakly singular integral operators. Note that the above formula includes only first-order derivatives of the basis and testing functions, whereas formula (20) in Ref. [20] includes second-order derivatives of the basis functions. This in turn means that the basis functions must be continuously differentiable in Ref. [20].

Next the boundary condition (2) is applied to BMIE (15). By replacing $\partial p/\partial n$ with $\eta p+g$ and by moving all known quantities to the right-hand side of the equation gives the final form of the integral equation

$$\left(\mathcal{K}-\frac{1}{2}\mathcal{I}\right)(p) - \mathcal{S}(\eta p) + \beta\left(\mathbf{n}\cdot\nabla\times\mathcal{S}(\mathbf{rot}'p) + k_0^2\mathcal{S}(\mathbf{n}\cdot\mathbf{n}'p) - \left(\mathcal{M}+\frac{1}{2}\mathcal{I}\right)(\eta p)\right) = (\mathcal{S}g) - p^{\mathrm{inc}} + \beta\left(\left(\mathcal{M}+\frac{1}{2}\mathcal{I}\right)(g) - \frac{\partial p^{\mathrm{inc}}}{\partial n}\right). \tag{17}$$

For more details and limitations of the above formulation we refer to Refs. [12,49].

3.2.2. Matrix equations

Next we write out the matrix equations of the weakly singular weak form of the BMIE (17). Let the surface S be divided into flat triangular elements and let the unknown pressure p be expressed by a linear combination

of continuous basis functions $u_n^{(q)}$, $n = 1, \ldots, N^{(q)}$, [50], defined on these elements as

$$p = \sum_{n=1}^{N^{(q)}} \alpha_n u_n^{(q)}. \tag{18}$$

Here $q = 1, 2$ or 3 is the order of a basis function u_n. In the sequel index q is omitted. The basis functions are introduced in the appendix. The main reason for using flat elements instead of curved ones, is that for flat triangular elements the singular parts of the integrals can be calculated in closed form [42]. The formulation of this paper is general (excluding the singularity extraction technique) and applies on curved elements, too.

A substitution of Eq. (18) into Eq. (17), using Galerkin testing procedure, i.e. using functions u_m, $m = 1, \ldots, N$, as testing functions, integrating over the surface S, and applying Eq. (16) on the third term on the left-hand side of Eq. (17) (the term including the curl), gives the following matrix equation:

$$[\mathbf{A} + \beta \mathbf{B}]\boldsymbol{\alpha} = \mathbf{b}^{(1)} + \beta \mathbf{b}^{(2)}, \tag{19}$$

where $\boldsymbol{\alpha} = [\alpha_1, \ldots, \alpha_N]^{\mathrm{T}}$ is the unknown coefficient vector. The elements of the matrices $\mathbf{A}$ and $\mathbf{B}$ are

$$\begin{aligned} \mathbf{A}_{mn} = & \int_S u_m(\mathbf{r}) \int_S \frac{\partial G}{\partial n'}(\mathbf{r}, \mathbf{r}') u_n(\mathbf{r}') \, \mathrm{d}S' \, \mathrm{d}S - \frac{1}{2} \int_S u_m(\mathbf{r}) u_n(\mathbf{r}) \, \mathrm{d}S \\ & - \int_S u_m(\mathbf{r}) \int_S G(\mathbf{r}, \mathbf{r}') \eta(\mathbf{r}') u_n(\mathbf{r}') \, \mathrm{d}S' \, \mathrm{d}S, \end{aligned} \tag{20}$$

$$\begin{aligned} \mathbf{B}_{mn} = & - \int_S \mathbf{rot}\, u_m(\mathbf{r}) \int_S G(\mathbf{r}, \mathbf{r}') \mathbf{rot}'\, u_n(\mathbf{r}') \, \mathrm{d}S' \, \mathrm{d}S + k_0^2 \int_S u_m(\mathbf{r}) \int_S (\mathbf{n} \cdot \mathbf{n}') G(\mathbf{r}, \mathbf{r}') u_n(\mathbf{r}') \, \mathrm{d}S' \, \mathrm{d}S \\ & - \int_S u_m(\mathbf{r}) \int_S \frac{\partial G}{\partial n}(\mathbf{r}, \mathbf{r}') \eta(\mathbf{r}') u_n(\mathbf{r}') \, \mathrm{d}S' \, \mathrm{d}S - \frac{1}{2} \int_S u_m(\mathbf{r}) \eta(\mathbf{r}) u_n(\mathbf{r}) \, \mathrm{d}S \end{aligned} \tag{21}$$

for all $m, n = 1, \ldots, N$, and the elements of the vectors $\mathbf{b}^{(1)}$ and $\mathbf{b}^{(2)}$ are

$$\mathbf{b}_m^{(1)} = \int_S u_m(\mathbf{r}) \left(\int_S G(\mathbf{r}, \mathbf{r}') g(\mathbf{r}') \, \mathrm{d}S' - p^{\mathrm{inc}}(\mathbf{r}) \, \mathrm{d}S \right), \tag{22}$$

$$\mathbf{b}_m^{(2)} = \int_S u_m(\mathbf{r}) \left(\int_S \frac{\partial G}{\partial n}(\mathbf{r}, \mathbf{r}') g(\mathbf{r}') \, \mathrm{d}S' + \frac{1}{2} g(\mathbf{r}) - \frac{\partial p^{\mathrm{inc}}}{\partial n}(\mathbf{r}) \right) \mathrm{d}S \tag{23}$$

for all $m = 1, \ldots, N$.

3.3. Evaluation of singular integrals

In this section the singularity extraction technique [18,19] is introduced for the numerical evaluation of the surface integral operators with singular kernels arising from the Galerkin-type discretization of the weakly singular BMIE. It has been demonstrated, e.g., in Refs. [51,43] that this method clearly improves the accuracy of the self-interaction terms of the system matrix, and thus, leads to a more stable algorithm than pure numerical integration, e.g. polar coordinate transform [17] or Duffy's method [16]. It should be pointed out that the method also improves the accuracy of the near-singular terms, not only the singular ones. In particular, the polar coordinate transform and Duffy's method are not accurate in the near-singular case, i.e. when the field point is close to the source point, but they do not coincide. In that case usually special techniques are required to improve the accuracy of the numerical method [52,53].

The idea of the singularity extraction technique is to subtract one or more singular terms from the integral kernel and integrate them in closed form. This method is originally introduced in Refs. [18,19], where analytical formulas for singular integrals of order $1/R$ and $1/R^2$ times a linear shape function over plane polygons were presented. In Ref. [54] the method was extended for more general integrals of order R^n, $n \geqslant -2$, times a linear vector basis functions in the context of electromagnetic applications so that more terms can be extracted from the kernel and integrated analytically. In Ref. [42] the method was further generalized for the high-order polynomial basis functions of arbitrary order.

Next we briefly consider the singularity extraction technique to evaluate the singular and near-singular integrals of the present BMIE formulation. For more details we refer to Ref. [42]. We note that the method presented here differs from the one applied earlier in acoustic problems, since, e.g. in Ref. [55] only the leading singularity times a constant function is integrated analytically.

The matrix elements in Eqs. (20)–(21) include the following singular integrals:

$$\int_S G(\mathbf{r},\mathbf{r}')w(\mathbf{r}')\,\mathrm{d}S', \quad \int_S \frac{\partial G}{\partial n'}(\mathbf{r},\mathbf{r}')w(\mathbf{r}')\,\mathrm{d}S' \tag{24}$$

and

$$\int_S \frac{\partial G}{\partial n}(\mathbf{r},\mathbf{r}')w(\mathbf{r}')\,\mathrm{d}S'. \tag{25}$$

Here the integration domain can be restricted to the support of the function w and w can be a scalar or a vector function, i.e. $w = f\,u_n$ or $w = \mathbf{rot}\,u_n$, respectively. Here $f = 1$, $f = \mathbf{n}\cdot\mathbf{n}'$ or $f = \eta$. The kernels of the above integrals become singular as $R = |\mathbf{r}-\mathbf{r}'| \to 0$. On the smooth surface they are weakly singular and behave as $\mathcal{O}(1/R)$ and on the non-smooth surfaces in the vicinity of edges and corners, the kernels of the integrals including derivatives of G become strongly singular and behave as $\mathcal{O}(1/R^2)$.

First the exponential function is expanded as a Taylor series with respect to R, and by using this, we write the Green's function as

$$G(R) = \frac{1}{4\pi}\sum_{l=0}^{\infty}\frac{(\mathrm{i}k)^l}{l!}R^{l-1}. \tag{26}$$

Next the Green's function is decomposed in two terms

$$G(R) = \left(G(R) - \frac{1}{4\pi}\sum_{l=0,2,\ldots}^{L}\frac{(\mathrm{i}k)^l}{l!}R^{l-1}\right) + \frac{1}{4\pi}\sum_{l=0,2,\ldots}^{L}\frac{(\mathrm{i}k)^l}{l!}R^{l-1}. \tag{27}$$

Since the odd terms with respect to l are smooth they can be omitted. The idea is to take L large enough so that the first term on the right-hand side inside the brackets is sufficiently regular and can be integrated efficiently with standard numerical methods, e.g. with Gaussian quadrature. The extracted terms, i.e. the components of the second term on the right-hand side, are such that they can be integrated in closed form over plane triangles. Usually it is sufficient to extract the first two or three even terms. With $L = 4$, for example, the Green's function is written as

$$G(R) = \left(G(R) - \frac{1}{4\pi R} + \frac{k^2 R}{8\pi} - \frac{k^4 R^3}{96\pi}\right) + \frac{1}{4\pi R} - \frac{k^2 R}{8\pi} + \frac{k^4 R^3}{96\pi}. \tag{28}$$

As an example, consider calculation of the third term of the matrix $\mathbf{A}$, see Eq. (20). Suppose that the basis functions are of order q. Since η is assumed to be constant in each element and the basis functions can be expressed in terms of the nodal shape functions of the corresponding order, see Eq. (38), we can write

$$\int_S G(\mathbf{r},\mathbf{r}')\eta(\mathbf{r}')u_n^{(q)}(\mathbf{r}')\,\mathrm{d}S' = \sum_{j=1}^{J}\eta_j\int_{T_j} G(\mathbf{r},\mathbf{r}')N_{nj}^{(q)}(\mathbf{r}')\,\mathrm{d}S', \tag{29}$$

where T_j, $j = 1,\ldots,J$, are the elements in which the basis function $u_n^{(q)}$ has non-zero values, η_j is the value of η in T_j and $N_{nj}^{(q)}$ is the qth-order nodal shape function of triangle T_j associated to a nodal point $\mathbf{p}_n$. Next writing the Green's function as in Eq. (28), the right-hand side of Eq. (29) becomes

$$\sum_{j=1}^{J}\eta_j\int_{T_j}\left(G(R) - \frac{1}{4\pi R} + \frac{k^2 R}{8\pi} - \frac{k^4 R^3}{96\pi}\right)N_{nj}^{(q)}(\mathbf{r}')\,\mathrm{d}S' + \sum_{j=1}^{J}\eta_j\int_{T_j}\left(\frac{1}{4\pi R} - \frac{k^2 R}{8\pi} + \frac{k^4 R^3}{96\pi}\right)N_{nj}^{(q)}(\mathbf{r}')\,\mathrm{d}S'. \tag{30}$$

Here the first integral is calculated numerically and the second one is calculated analytically with the formulas given in Ref. [42]. The same procedure applies to the second term of the matrix $\mathbf{B}$ in Eq. (21), too, since $\mathbf{n}\cdot\mathbf{n}'$ is constant in T_j.

Terms including gradient of the Green's function are considered similarly, by replacing each term in Eq. (28) with its gradient. Thereafter, the normal derivatives required in Eqs. (24) and (25) are obtained by taking normal components. Terms including **rot** u_n are considered by differentiating the nodal shape functions. Since the derivatives of the polynomial nodal shape functions are also polynomial, these terms can be integrated as terms including u_n.

After the integrals with respect to $\mathbf{r}'$ are evaluated, the integrals with respect to $\mathbf{r}$ are usually sufficiently regular and can be evaluated with standard numerical quadratures. More integration points are required for small R. Note that if $l=-2$, $\mathbf{r}$ is not allowed to be in the integration domain. These terms appear in computing the gradient of the Green's function. Fortunately, the kernel $\mathbf{n}\cdot\nabla G$ vanishes for planar elements when both $\mathbf{r}$ and $\mathbf{r}'$ are on the same element. When the field and source points are on the adjacent elements, which are not in the same plane, this kernel becomes strongly singular as $R\to 0$. In that case the singularity extraction technique clearly improves numerical efficiency and more accurate results with a lower computational cost can be obtained, than with pure numerical methods.

Finally, we note that the singularity extraction technique should be applied only when R is small, e.g. smaller than $\lambda/5$, where λ is the wavelength. For large R the integrands are smooth and can be evaluated with standard numerical methods. Note also that the method is independent on the location of the points $\mathbf{r}$ and $\mathbf{r}'$ and it works similarly in the singular and near-singular cases.

4. Iterative solution and preconditioning

In this section we consider solution of matrix equation (19). Since discretization of an integral equation leads to a dense linear system, for problems with fairly high number of unknowns, direct methods such as Gaussian elimination become very expensive with respect to both computing time and memory requirements. Hence, large systems should be solved with iterative methods, e.g. with Krylov subspace methods [56,22,23]. However, in many cases the convergence of an iterative solver may be rather poor leading to a long computing time. The convergence rate can be increased by preconditioning.

In this section we present a simple and efficient incomplete LU (ILU) preconditioner for the linear system arising from the high-order Galerkin discretization of the BMIE formulation. Similar preconditioner has been applied previously in Ref. [27] with discontinuous basis functions and point collocation.

Let us denote the matrix equation (19) shortly as follows:

$$\mathbf{M}\boldsymbol{\alpha}=\mathbf{b}. \tag{31}$$

Since the system matrix $\mathbf{M}$ is complex and non-symmetric, the generalized minimal residual method (GMRES) [23] is applied to solve the system iteratively. The GMRES method has been also found to be the most robust iterative solvers in many exterior acoustic problems [26]. We seek such a preconditioner matrix $\mathbf{P}$ that the system

$$\mathbf{M}\mathbf{P}^{-1}\mathbf{w}=\mathbf{b} \tag{32}$$

with $\boldsymbol{\alpha}=\mathbf{P}^{-1}\mathbf{w}$ leads to a faster convergence with an iterative solver than the original system (31) and $\mathbf{P}^{-1}$ is cheap to compute and store. The ILU preconditioner is built using the diagonal and nearby terms of $\mathbf{M}$ as follows: First we pick the nearby terms of the matrix $\mathbf{M}$ that correspond to topologically close nodes. More precisely, if nodes i and j belong to the same element then the matrix element $\mathbf{M}_{ij}$ is chosen. Let $\tilde{\mathbf{M}}$ denote the matrix composed by these elements. This matrix is structurally symmetric and sparse. Next permutation matrix $\mathbf{Q}$ is applied to minimize the fill-in of the LU decomposition. The incomplete LU decomposition (sparse approximation for the LU decomposition) with the ILUT-algorithm [44] is generated for $\tilde{\mathbf{M}}$

$$\mathbf{Q}^{\mathrm{T}}\tilde{\mathbf{M}}\mathbf{Q}\approx\mathbf{L}\mathbf{U}. \tag{33}$$

The ILUT threshold τ is set to value 10^{-3}. The permutation matrix $\mathbf{Q}$ is obtained with the Sloan algorithm [57,58]. Other possibilities are, e.g. reverse Cuthill–McKee and nested dissection algorithms [44]. System (32) is then solved iteratively with the GMRES method by first solving $\mathbf{w}$ from

$$\mathbf{Q}^{\mathrm{T}}\mathbf{M}\mathbf{Q}\,(\mathbf{L}\mathbf{U})^{-1}\mathbf{w}=\mathbf{Q}^{\mathrm{T}}\mathbf{b} \tag{34}$$

and then computing $\boldsymbol{\alpha}$ from

$$\boldsymbol{\alpha} = \mathbf{Q}(\mathbf{LU})^{-1}\mathbf{w}. \tag{35}$$

For N unknowns and for dense matrix equations, both the memory and CPU time requirements of an iterative solver are still $\mathcal{O}(N^2)$, making it rather impractical for large problems. In order to further reduce the computational cost, an iterative solver should be combined with a fast solution procedure, such as the fast multipole method (FMM).

5. Numerical examples

In this section the developed method is verified by numerical examples. First, acoustic scattering by a sphere with the impedance boundary condition is considered and the results are validated by making comparisons with analytical series expansion solutions. Then the convergence of GMRES(25) method (restart after 25 iterations) with and without the ILU preconditioner is studied. In all examples we have set $g = 0$ in Eq. (2) and the source of an incident sound wave is generated by a point source at point $\mathbf{r}_0$:

$$p^{\text{inc}}(\mathbf{r}) = \frac{C}{4\pi}\frac{\mathrm{e}^{\mathrm{i}k_0|\mathbf{r}-\mathbf{r}_0|}}{|\mathbf{r}-\mathbf{r}_0|}, \tag{36}$$

where C is a constant. The stopping criterion for the GMRES method is

$$\frac{\|\hat{\mathbf{M}}\boldsymbol{\alpha}_n - \hat{\mathbf{b}}\|_2}{\|\hat{\mathbf{b}}\|_2} < \text{tol}, \tag{37}$$

where tol is a given error tolerance, $\hat{\mathbf{M}}$ and $\hat{\mathbf{b}}$ are the system matrix and excitation vector of the preconditioned system (34) (or of the original system (31) if preconditioner is not used) and $\boldsymbol{\alpha}_n$ is the solution at the nth iteration step.

5.1. Verification

Consider first acoustic scattering by a sphere with the radius $a = \pi/k_0$. This radius corresponds to the first interior resonance of the sphere. The frequency is 1700 Hz. The incident wave is generated by a point source at point $(10\,a, 0, 0)$ with $C = 1$. On the surface of the sphere we apply the Neumann boundary condition $(\partial p/\partial n = 0)$ and the impedance boundary conditions $\partial p/\partial n = \eta p$ with $\eta = 10, 10 - 10\mathrm{i}$ and $\eta = 10\,000$, respectively. The last case approximates the Dirichlet boundary condition $(p = 0)$.

Fig. 1 shows the angular dependence of the scattered pressure along a circle of radius $r = 5a$ on the (x, y)-plane. The analytic spherical wave series expansion solutions are included in the figure. In the case $\eta = 10\,000$ the analytical solution is obtained with the Dirichlet boundary condition. The figures show that the BMIE formulation is free of the interior resonances and that the solutions agree well with the analytical ones. The solutions of Fig. 1 are obtained with 1442 first-order basis functions and the surface of the sphere is divided into 2880 planar triangles. In all cases the GMRES method with the stopping criterion $\text{tol} = 10^{-6}$ and ILU preconditioner converged in 10–15 iterations.

5.2. Convergence results

Next we study the convergence of GMRES method with and without the ILU preconditioner more systematically. The number of iterations depends on many factors such as (see also Ref. [26]):

(1) geometry of the object and boundary condition,
(2) frequency,
(3) excitation,
(4) integral equation formulation,
(5) basis and testing functions,
(6) discretization,

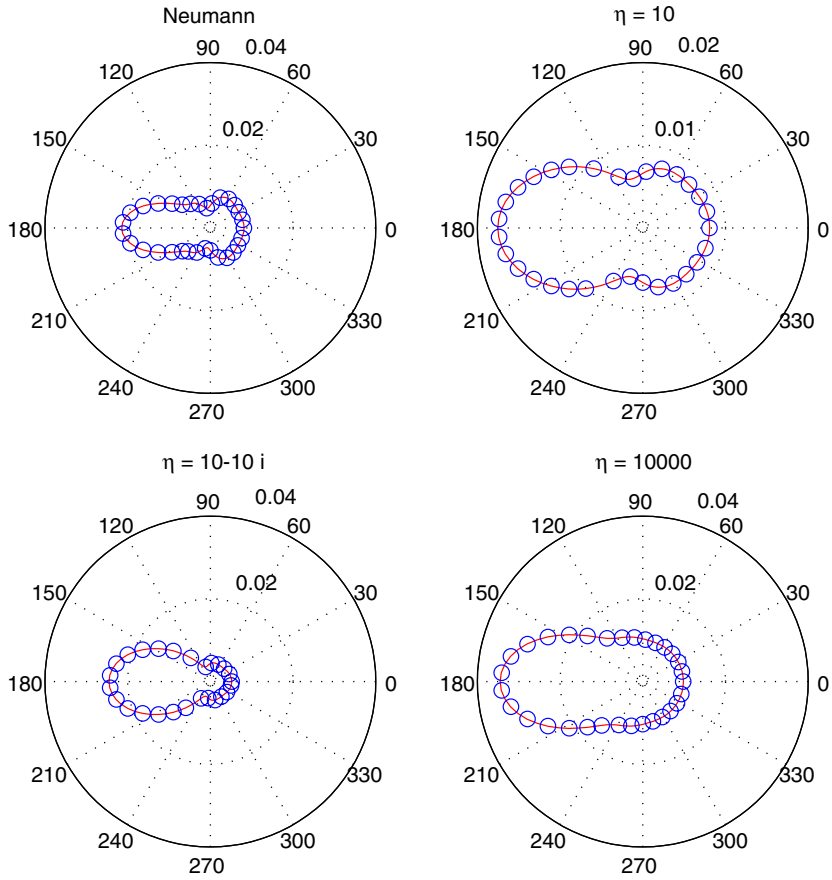

Fig. 1. Angular dependence of the scattered pressure at a circle of radius $5a$ for a sphere of radius $a = \pi/k_0$ with the Neumann boundary condition ($\eta = 0$) and three impedance boundary conditions. Analytical solutions are denoted by solid lines and numerical solutions are denoted by circles.

(7) iterative solver and initial guess,
(8) preconditioning.

In this section we focus on the effect of items (1), (2), (5) and (8) on the convergence of the GMRES method. In all cases the initial guess for the GMRES method is a zero vector. In addition, we study the effect of the coupling parameter β of the BMIE formulation on the convergence rate, too.

Let us begin by considering scattering by a rigid sphere. Radius of the sphere a is varied from $0.01\,\pi/k_0$ to $5\pi/k_0$. Table 1 shows the relative L_2 error of the numerical solution calculated at 100 points on a circle of radius $r = 5a$ on the (x, y)-plane when a unit point source ($C = 1$) is at point $(10a, 0, 0)$. The discretization is the same as in the previous section. In addition, Table 1 shows the number of iterations of the GMRES method required to obtain relative residual error of 10^{-6} with and without the ILU preconditioner, and the approximate number of elements per wavelength. For low size parameters $k_0 a < 1$, i.e. for low frequencies when the size of the sphere is fixed, the error in the solution is mostly due to the error made in approximating a sphere with planar triangles. The results show that the preconditioner has a higher effect on the convergence rate on the high frequencies. However, the differences on the results are rather small and the number of iterations is almost constant in all considered cases. We may conclude that the BMIE formulation leads to rapidly converging iterative solutions on a wide frequency range.

Next we study the effect of the coupling parameter β on the convergence rate. Again we consider a rigid sphere. Table 2 lists the number of iterations with tol $= 10^{-6}$ and the ILU preconditioner as a function of the coupling parameter β and the size parameter $k_0\,a$. The mesh and basis functions are the same as in the previous

Table 1
The relative error of the numerical solution, the number of iterations of the GMRES with and without the ILU preconditioner, N_{iter} (ILU) and N_{iter}, respectively, and the approximate number of elements per wavelength λ for a rigid sphere of radius a with 1442 first-order basis functions

ka/π	Error (%)	N_{iter} (ILU)	N_{iter}	Elements/λ
1/100	0.38	13	16	2130
1/50	0.38	13	16	1065
1/10	0.37	14	17	213
1/5	0.34	14	17	107
1	0.46	14	18	22
2	0.68	13	19	11
3	0.95	12	18	7
4	1.32	11	19	5.5
5	1.90	11	19	4

Table 2
The number of iterations of the GMRES with the ILU preconditioner as a function of the coupling parameter $\beta = (0, \ldots, i)$ and size parameter k_0a for a rigid sphere of radius a with 1442 first-order basis functions

ka/π	0	0.002i	0.004i	0.02i	0.04i	0.2i	0.4i	0.6i	0.8i	i
1/100	4	**13**	14	16	18	19	19	20	20	20
1/50	4	12	**13**	15	16	18	19	19	19	19
1/10	4	9	11	**14**	15	16	17	17	17	17
1/5	5	8	9	13	**15**	16	16	16	16	16
1	10	10	11	12	**15**	19	20	20	20	20
2	18	15	15	12	**14**	26	31	33	35	35
3	33	24	22	12	**13**	32	42	45	47	50
4	44	31	26	13	**12**	32	46	56	60	64
5	57	42	32	13	**11**	31	49	62	71	78

Table 3
Optimal coupling parameter β suggested by Eq. (12) for various size parameters k_0a in the case of a sphere with radius a

k_0a/π	β
1/100	0.002i
1/50	0.004i
1/10	0.02i
$>1/10$	0.038i

examples. The (non-zero) values of β are chosen so that they satisfy $\beta = 2ia$ for radii $a = 0.01\pi/k_0, \ldots, 5\pi/k_0$. The results show that at low frequencies, $k_0a/\pi < 1$, the fastest convergence is obtained with $\beta = 0$. At higher frequencies $\beta = 0$, however, it is not a proper choice, since it results in the integral equation formulation which does not have unique solution for all frequencies. For $k_0a/\pi \geqslant 1$ the choices $\beta = 0.02$i and 0.04i seem to give the fastest convergence rates. It is also interesting to see that for $k_0a/\pi \geqslant 1$ increasing β results in slower convergence. The values suggested by Eq. (12) and used on the other calculations of this paper are given in Table 3. The iteration counts corresponding to these values are indicated in Table 2 with boldface.

Then we study convergence of the GMRES method when the number of unknowns is varied. Table 4 lists the number of iterations as a function of the size parameter k_0a and the number of unknowns with preconditioning. Again we consider a rigid sphere with the first-order basis functions. For comparison Table 5 shows the same results without the preconditioner. These results, together with the results of Table 1, show an

Table 4
The number of iterations of the GMRES with the preconditioner as a function of $k_0a/\pi(=1/100, 1/50, \ldots, 5)$ and number of unknowns for a rigid sphere of radius a with the first-order basis functions

Unknowns	1/100	1/50	1/10	1/5	1	2	3	4	5
1002	12	12	12	13	13	12	11	11	10
1442	13	13	14	14	14	13	12	11	11
1962	14	14	15	15	15	14	13	12	12
2562	15	15	16	17	16	15	13	12	12
3242	16	16	17	18	17	16	14	13	12
4002	17	17	18	19	18	16	15	13	13

Table 5
The number of iterations of the GMRES without the preconditioner as a function of $k_0a/\pi(=1/100, 1/50, \ldots, 5)$ and number of unknowns for a rigid sphere of radius a with the first-order basis functions

Unknowns	1/100	1/50	1/10	1/5	1	2	3	4	5
1002	14	14	15	16	17	18	18	19	19
1442	16	16	17	17	18	19	18	19	19
1962	17	17	18	19	19	20	19	19	19
2562	18	18	19	20	20	20	19	19	19
3242	19	20	21	21	21	21	20	19	19
4002	21	21	22	22	22	22	20	20	20

Table 6
The number of iterations of the GMRES with the preconditioner as a function of $k_0l/\pi(=1/100, 1/50, \ldots, 5)$ and the number of unknowns for a rigid cube of side length l with the first-order basis functions

Unknowns	1/100	1/50	1/10	1/5	1	2	3	4	5
866	14	15	16	16	15	13	12	12	12
1178	16	16	18	17	16	14	13	13	12
1946	18	18	20	19	18	15	15	14	13
2906	20	20	22	21	20	17	16	15	14
4058	21	22	24	23	21	18	17	16	15
5402	23	24	25	24	23	20	18	17	16

Table 7
The number of iterations of the GMRES with the preconditioner as a function of $k_0l/\pi(=1/100, 1/50, \ldots, 5)$ and the number of unknowns for a rigid cube of side length l with the second-order basis functions

Unknowns	1/100	1/50	1/10	1/5	1	2	3	4	5
866	14	15	16	15	15	13	12	12	12
1538	17	17	18	17	17	15	14	13	13
2402	19	19	20	20	19	16	15	14	14
3458	21	21	22	21	20	18	17	16	15
4706	22	23	24	23	21	19	18	17	16

important feature of the BMIE formulation: the number of iterations increases very slowly as the number of unknowns (per wavelength) is increased.

Next we study the effect of increasing the order of the basis functions on the convergence rate of the GMRES method with preconditioning. We consider a rigid, cube with the side length l and faces parallel to the coordinate axis. Center of the cube is at the origin and a unit point source is at point $(10l, 0, 0)$. Tables 6–8

Table 8
The number of iterations of the GMRES with the preconditioner as a function of $k_0 l/\pi (= 1/100, 1/50, \ldots, 5)$ and the number of unknowns for a rigid cube of side length l with the third-order basis functions

Unknowns	1/100	1/50	1/10	1/5	1	2	3	4	5
866	14	15	16	15	14	13	12	12	12
1946	17	18	19	19	17	15	14	13	13
3458	20	20	22	21	19	17	16	15	14
5402	22	23	24	23	21	19	18	17	16

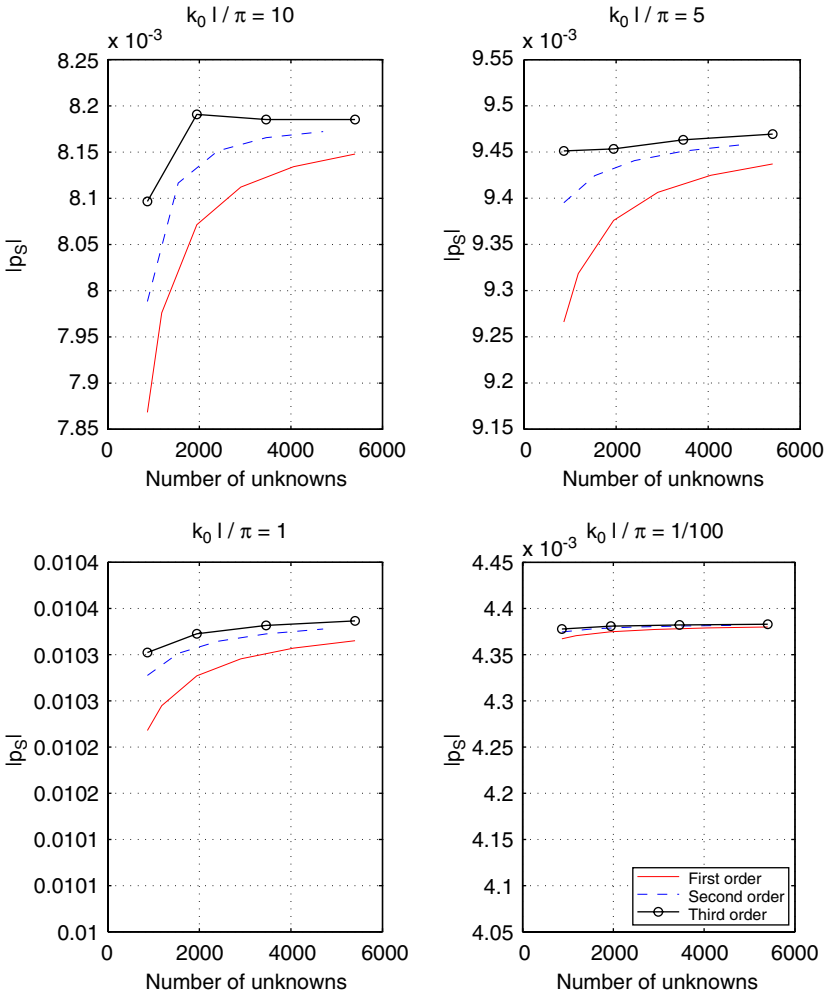

Fig. 2. The back-scattered secondary pressure at point $(5l, 0, 0)$ for various size parameters $k_0 l$ with the first-(solid line), second-(dashed line) and third-(solid line with circles) order basis functions as a function of number of unknowns for a rigid cube of size length l.

show the number of iterations required to obtain relative residual error of 10^{-6} as a function of number of unknowns and the size parameter $k_0 l$. The results indicate that the number of iterations is almost the same for the applied first-, second- and third-order basis functions with the same number of unknowns.

Next we study the effect of increasing the order of the basis functions on the solution accuracy. Fig. 2 shows the back-scattered pressure at point $(5l, 0, 0)$ as a function of number of unknowns with the first-, second- and

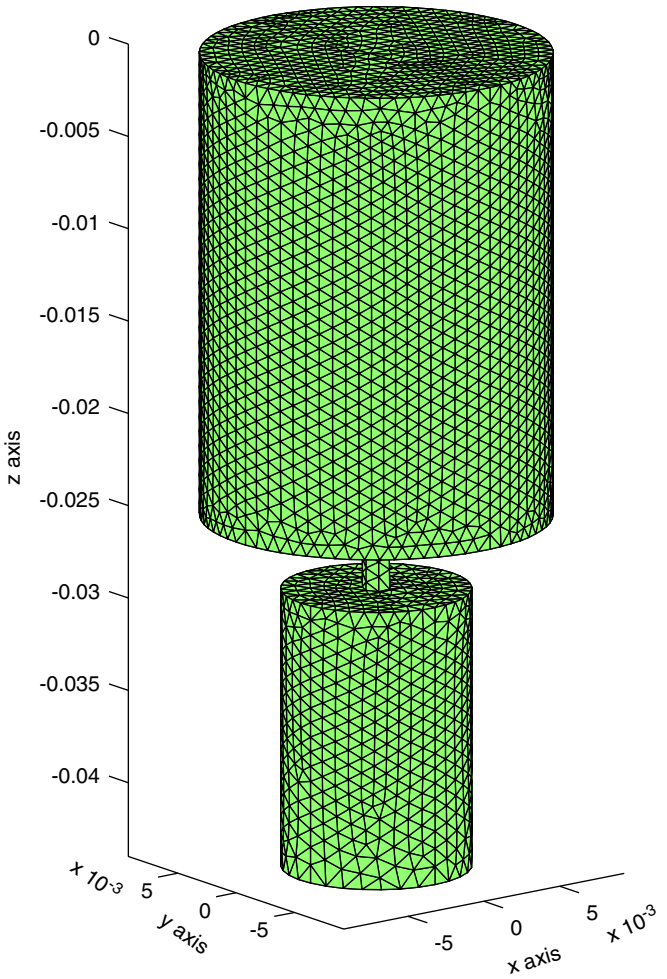

Fig. 3. Triangularization of a cylindrical object. The dimensions are in meters.

third-order basis functions for the same rigid cube as in the previous example. The results show that using high-order basis functions the solution converges more rapidly with respect to the number of unknowns than when the first-order basis functions are applied. In particular, this is true at high frequencies $k_0 l/\pi > 1$.

Finally we consider two more irregular objects. The first one consists of two circular cylinders with radii 9.25 mm (top), 5 mm (bottom) and heights 25 mm (top), 15 mm (bottom), respectively. The cylinders are connected by a thin cylindrical tube of radius 0.7 mm and height 4 mm. The triangularization of the object (8819 planar triangles) is displayed in Fig. 3 and the number of unknowns with the first-order basis functions is 4461. A unit point source is at point $(0, 0, 10)$ mm. The first three columns of Table 9 list the number of iterations with and without the preconditioner, for the Neumann boundary condition and for the impedance boundary conditions $\eta = 10, -10\mathrm{i}, 10 - 10\mathrm{i}$ and 10 000, respectively, when the frequency is 20 kHz. At that frequency the height of the object (44 mm) is roughly 2.5 wavelengths. Here $\mathrm{tol} = 10^{-6}$. The last four columns of Table 9 show the results with the Neumann boundary condition at various frequencies.

Second irregular object is the "cat's eye" considered earlier, e.g. in Refs. [59,26]. The object is a sphere with one octant cut out. Radius of the sphere $a = 1$ m and a unit point source is at point $(10a, -10a, 10a)$. Triangularization of the object with 4036 planar triangles is displayed in Fig. 4. Tables 10 and 11 show the number of GMRES iterations with and without ILU preconditioner as a function of boundary condition and frequency with 2405 (4806 triangles) and 4269 (8534 triangles) first-order basis functions, respectively.

Table 9
The number of iterations of the GMRES with and without the preconditioner N_{iter} (ILU) and N_{iter}, respectively, for the object of Fig. 3 with 4461 first-order basis functions

η	N_{iter} (ILU)	N_{iter}	f (Hz)	N_{iter} (ILU)	N_{iter}	Height/λ
0	21	31	100	31	60	0.013
10	20	30	500	31	62	0.065
-10i	21	31	1000	32	64	0.13
10-10i	20	30	5000	28	41	0.65
10 000	17	32	10 000	25	37	1.3

Columns 1–3 give the results for various boundary conditions at 20 kHz. Columns 4–6 give the results with the Neumann boundary condition for various frequencies. The last column shows the height of the object in terms of the wavelength λ for various frequencies.

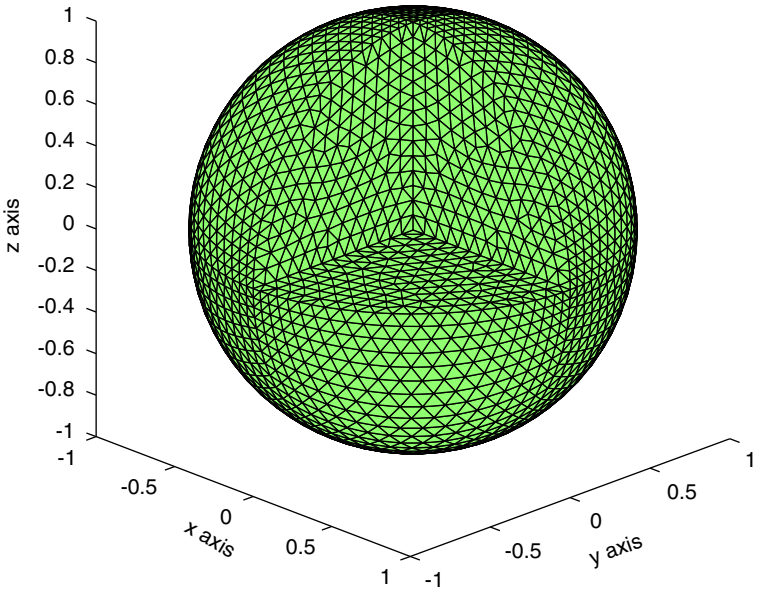

Fig. 4. Triangularization of the "cat's-eye" with 4806 planar triangles. The dimensions are in meters.

The last two examples further verify the impression that the BMIE formulation has very good properties when the matrix equation is solved iteratively with the GMRES method and high convergence rates can be obtained for various boundary conditions on a broad frequency range, although the results are not as good as they are in the case of regular objects like a sphere or a cube. The good convergence rates even at (very) low frequencies imply that the BMIE formulation is not plagued with the problem which is known as the low-frequency breakdown and which is a serious problem in the surface integral equation methods in electromagnetics [60]. It is worth noticing that this problem may occur at higher frequencies too if the discretization of the object includes elements which are very small compared to the wavelength. Very small elements are required, e.g. if the object under consideration includes tiny details which are important for the performance of the device and thus, require accurate modelling.

In all considered examples the number of unknowns has been rather low (less than 5500) for a realistic application of iterative methods, (in all cases we can solve the system with a direct solver in a standard PC), and the CPU time required to solve the system, as well as time and memory required in building the ILU preconditioner, are rather small compared to the time required to compute the matrix elements. With the higher number of unknowns, the number of iterations will play a more crucial role in the total computation time. In particular, this is the case when iterative methods are combined with fast solution procedures, like the multilevel fast multipole algorithm (MLFMA), where only the near field terms of the system matrix are

Table 10
The number of iterations of the GMRES with and without the preconditioner, N_{iter} (ILU) and N_{iter}, respectively, for the cat's eye with 2405 first-order basis functions

η	N_{iter} (ILU)	N_{iter}	f (Hz)	N_{iter} (ILU)	N_{iter}	k_0a
0	21	28	100	21	27	1.85
10	17	21	250	21	28	4.62
-10i	20	27	500	21	27	9.24
10-10i	16	22	750	20	27	13.86
10 000	13	31	1000	20	28	18.48

Columns 1–3 give the results for various boundary conditions with $k_0a = \pi$ and columns 4–6 give the results with the Neumann boundary condition for various frequencies. The last column shows the size parameter k_0a for various frequencies, where a is the radius of the sphere.

Table 11
The number of iterations of the GMRES with and without the preconditioner, N_{iter} (ILU) and N_{iter}, respectively, for the cat's eye with 4269 first-order basis functions, similarly as in Table 10

η	N_{iter} (ILU)	N_{iter}	f (Hz)	N_{iter} (ILU)	N_{iter}	k_0a
0	24	35	100	24	31	1.85
10	19	24	250	25	32	4.62
-10i	23	32	500	24	35	9.24
10-10i	19	25	750	24	34	13.86
10 000	14	31	1000	24	35	18.48

computed with numerical integration and the far field terms are calculated by an approximative scheme. As the numerical examples clearly show (Tables 4–8), the number of iterations increases very slowly as the number of unknowns is increased. Our preliminary results with tens of thousands of unknowns (and MLFMA) have verified this argument.

6. Conclusions

In this paper a high-order boundary element method for solving time harmonic acoustic scattering problems with the impedance boundary condition is presented. The method is based on the Galerkin-type formulation of the Burton Miller integral equation (BMIE) with continuous high-order basis and testing functions. With the Galerkin method the hypersingular operator of the traditional BMIE formulation can be avoided, thus making the numerical implementations more efficient and straightforward than with the point collocation method. The singular and near-singular integrals of the BMIE formulation are evaluated with the singularity extraction technique. By this method the near interaction terms of the system matrix are evaluated with a high accuracy, thus leading to a more stable and robust method than by using pure numerical integration quadratures (e.g. polar coordinate transform).

The resulting matrix equation is solved iteratively with the restarted version of the GMRES algorithm. A simple ILU preconditioner is developed to speed up the convergence and to reduce the number of required iterations. Several numerical examples demonstrate the good properties of the BMIE formulation with iterative solvers and the efficiency of the preconditioner. The BMIE with the Galerkin method and high-order basis functions leads to rapidly converging iterative solvers for various boundary conditions and geometries on a broad frequency range. Hence, the BMIE formulation is well suited for an efficient application of fast methods, like the MLFMA. Also the developed ILU preconditioner would be directly available in the MLFMA implementations since it is built using only the nearby terms of the system matrix.

Acknowledgements

The authors wish to thank Asta and Leo Kärkkäinen, Nokia Research Center, Helsinki, Finland, for a very pleasant collaboration during this work.

Appendix Basis functions

In this appendix we introduce the applied high-order basis functions. We use node-based basis functions. The first-, second- and third-order basis functions are defined so that they are polynomials of the corresponding order and they have value one at one node point of the mesh and zero on the other points. In addition, the basis functions are defined so that they are continuous over the element boundaries. The basis functions of order q associated to a node point $\mathbf{p}_n$ can be represented at a point $\mathbf{r}$ on the surface as follows:

$$u_n^{(q)}(\mathbf{r}) = \sum_{j=1}^{J} N_{nj}^{(q)}(\mathbf{r}), \tag{38}$$

where $N_{nj}^{(q)}$ is the nodal shape function of order q associated to the node point $\mathbf{p}_n$ and defined on an element T_j. Here J is the number of elements in which the basis function $u_n^{(q)}$ is non-zero. Note that the nodal shape functions are non-zero only on one single element and, thus, the basis functions on each element are defined by the nodal shape functions of that element only.

The node points for the first-, second- and third-order shape functions $N^{(1)}, N^{(2)}$ and $N^{(3)}$ are displayed in Figs. 5–7, respectively. In addition, the second- and third-order nodal shape functions can be defined, respectively, on a plane triangle in terms of the first-order shape functions $N_1^{(1)}, N_2^{(1)}$ and $N_3^{(1)}$ by [50, p. 2.125]

$$\begin{aligned} N_{2n-1}^{(2)} &= 2N_n^{(1)}(N_n^{(1)} - \tfrac{1}{2}), \\ N_{2n}^{(2)} &= 4N_n^{(1)}N_{n+1}^{(1)} \end{aligned} \tag{39}$$

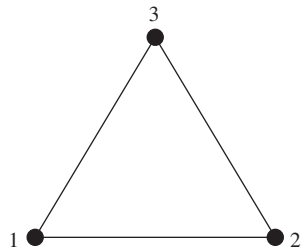

Fig. 5. An element with linear shape functions.

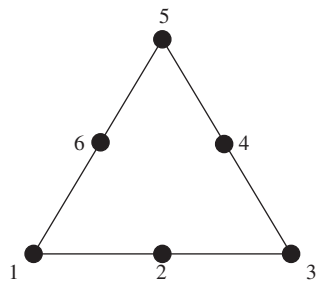

Fig. 6. An element with second-order shape functions.

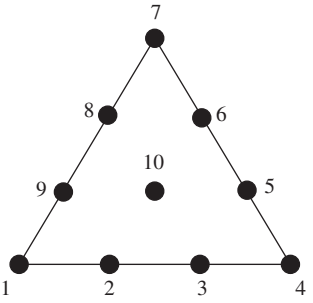

Fig. 7. An element with third-order shape functions.

and

$$
\begin{aligned}
N^{(3)}_{3n-2} &= \tfrac{1}{2}(3N^{(1)}_n - 1)(3N^{(1)}_n - 2)N^{(1)}_n,\\
N^{(3)}_{3n-1} &= \tfrac{9}{2}N^{(1)}_n N^{(1)}_{n+1}(3N^{(1)}_n - 1),\\
N^{(3)}_{3n} &= \tfrac{9}{2}N_n N^{(1)}_{n+1}(3N^{(1)}_{n+1} - 1),\\
N^{(3)}_{10} &= 27\,N^{(1)}_1 N^{(1)}_2 N^{(1)}_3
\end{aligned}
\tag{40}
$$

for $n = 1, 2, 3$. Here we have omitted the element numbers and $N^{(1)}_4 = N^{(1)}_1$.

References

[1] D. Colton, R. Kress, *Integral Equation Methods in Scattering Theory*, Wiley, New York, 1983.

[2] H.A. Schenck, Improved integral formulation for acoustic radiation problems, *Journal of Acoustic Society of America* 44 (1) (1968) 41–58.

[3] G.W. Benthien, H.A. Schenck, Nonexistence and nonuniqueness problems associated with integral equation method in acoustic, *Computer and Structures* 65 (1997) 295–305.

[4] I.L. Chen, J.T. Chen, M.T. Liang, Analytical study and numerical experiments for radiation and scattering problems using the CHIEF method, *Journal of Sound and Vibration* 248 (5) (2001) 809–828.

[5] I.L. Chen, J.T. Chen, S.R. Kuo, M.T. Liang, A new method for true and spurious eigensolutions of arbitrary cavities using the combined Helmholtz exterior integral equation formulation, *Journal of Acoustic Society of America* 109 (3) (2001) 982–998.

[6] A.J. Burton, G.F. Miller, The application of integral equation methods to numerical solutions of some exterior boundary value problem, *Proceedings of the Royal Society London Series A* 323 (1971) 210–210.

[7] C.C. Chien, H. Rajiyah, S.N. Atluri, An effective method for solving hypersingular integral equations in 3-D acoustic wave problems, *Journal of Acoustic Society of America* 88 (1990) 918–937.

[8] M. Tanaka, V. Sladek, J. Sladek, Regularization techniques applied to boundary element methods, *Applied Mechanical Review* 47 (1994) 457–499.

[9] Y.J. Liu, F.J. Rizzo, A weakly singular form of the hypersingular boundary integral equation applied to 3-D acoustics wave problems, *Computer Methods in Applied Mechanics and Engineering* 96 (1996) 271–287.

[10] W.S. Hwang, Hypersingular boundary integral equations for exterior acoustic problems, *Journal of Acoustic Society of America* 101 (6) (1997) 3330–3335.

[11] Y. Liu, S. Chen, A new form of the hypersingular boundary integral equation for 3-D acoustics and its implementation with C^0 boundary elements, *Computer Methods in Applied Mechanics and Engineering* 173 (1999) 375–386.

[12] L. Demkowicz, A. Karafiat, J. T. Oden, Variational (weak) form of the hypersingular formulation for the Helmholtz exterior boundary-value problems, TICOM Report 91-05, The Texas institute for Computational Mechanics, 1991.

[13] L. Demkowicz, J.T. Oden, Application of *hp*-adaptive BE/FE methods to elastic scattering, *Computer Methods in Applied Mechanics and Engineering* 133 (1996) 287–317.

[14] Y.C. Chang, L. Demkowicz, Solution of viscoelastic scattering problems in linear acoustics using *hp* boundary/finite element method, *International Journal for Numerical Methods in Engineering* 44 (1999) 1885–1907.

[15] P. Geng, J.T. Oden, R.A. Van den Geijn, Massively parallel computation for acoustical scattering problems using boundary element methods, *Journal of Sound and Vibration* 191 (1) (1996) 145–165.

[16] M.G. Duffy, Quadrature over a pyramid or cube of integrands with a singularity at a vertex, *SIAM Journal of Numerical Analysis* 19 (1982) 1260–1262.

[17] C. Schwab, W.L. Wendland, On numerical cubatures of singular surface integrals in boundary element methods, *Numerische Mathematik* 62 (1992) 343–369.

[18] D.R. Wilton, S.M. Rao, A.W. Glisson, D.H. Schaubert, O.M. Al-Bundak, C.M. Butler, Potential integrals for uniform and linear source distributions on polygonal and polyhedral domains, *IEEE Transactions on Antennas and Propagation* 32 (1984) 276–281.
[19] R.D. Graglia, On the numerical integration of the linear shape functions times the 3-D Green's function or its gradient on a plane triangle, *IEEE Transactions on Antennas and Propagation* 41 (1993) 1448–1455.
[20] M. Gennaretti, A. Giordani, L. Morino, A third-order boundary element method for exterior acoustics with applications to scattering by rigid and elastic shells, *Journal of Sound and Vibration* 222 (5) (1999) 699–722.
[21] P.J. Harris, K. Chen, On efficient preconditioners for iterative solution of a Galerkin boundary element equation for the three-dimensional exterior Helmholtz equation, *Journal of Computational and Applied Mathematics* 156 (2003) 303–318.
[22] R.W. Freund, Conjugate gradient-type methods for linear systems with complex symmetric matrices, *SIAM Journal of Scientific and Statistical Computing* 13 (1992) 425–448.
[23] Y. Saad, M.H. Schultz, GMRES: a generalized minimal residual algorithm for solving nonsymmetric linear systems, *SIAM Journal of Scientific and Statistical Computing* 7 (1986) 856–869.
[24] S. Amini, N.D. Maines, Preconditioned Krylov subspace methods for boundary element solution of the Helmholtz equation, *International Journal for Numerical Methods in Engineering* 41 (1998) 875–898.
[25] K. Chen, P.J. Harris, Efficient preconditioners for iterative solution of the boundary element equations for the three-dimensional Helmholtz equation, *Applied Numerical Mathematics* 36 (2001) 475–489.
[26] S. Marburg, S. Schneider, Performance of iterative solvers for acoustic problems: Part I: solvers and effect of diagonal preconditioning, *Engineering Analysis with Boundary Elements* 27 (2003) 727–750.
[27] S. Schneider, S. Marburg, Performance of iterative solvers for acoustic problems, Part II: acceleration by ILU-type preconditioner, *Engineering Analysis with Boundary Elements* 27 (2003) 751–757.
[28] M. Ochmann, A. Homm, S. Makarov, S. Semenov, An iterative GMRES-based boundary element solver for acoustic scattering, *Engineering Analysis with Boundary Elements* 27 (2003) 717–725.
[29] K. Chen, On a class of preconditioning methods for dense linear systems from boundary elements, *SIAM Journal of Scientific and Statistical Computing* 20 (1998) 684–698.
[30] S.A. Vavasis, Preconditioning for boundary integral equations, *SIAM Journal of Matrix Analysis and Applications* 13 (2000) 905–925.
[31] V. Rokhlin, Rapid solution of integral equations of scattering theory in two dimensions, *Journal of Computational Physics* 38 (1990) 414–439.
[32] C.-C. Lu, W.C. Chew, A multilevel algorithm for solving a boundary integral equation of wave scattering, *Microwave and Optical Technology Letters* 7 (10) (1994) 466–470.
[33] E. Bleszynski, M. Bleszynski, T. Jaroszewicz, AIM: adaptive integral method for solving large-scale electromagnetic scattering and radiation problems, *Radio Science* 31 (5) (1996) 1225–1251.
[34] J.R. Phillips, J.K. White, A precorrected-FFT method for electrostatic analysis of complicated 3-D structures, *IEEE Transactions of Computer-Aided Design of Integrated Circuits and Systems* 16 (10) (1997) 1059–1072.
[35] S. Schneider, Application of fast methods for acoustic scattering and radiation problems, *Journal of Computational Acoustics* 11 (3) (2003) 387–401.
[36] S. Amini, A.T.J. Profit, Multi-level fast multipole solution of the scattering problem, *Engineering Analysis with Boundary Elements* 27 (2003) 547–564.
[37] M. Fischer, U. Gauger, L. Gaul, A multipole Galerkin boundary element method for acoustics, *Engineering Analysis with Boundary Elements* 28 (2004) 155–162.
[38] O.P. Bruno, L.A. Kunyansky, Surface scattering in three dimensions: an accelerated high-order solver, *Proceedings of Royal Society of London A* 457 (2001) 2921–2934.
[39] E. Darrigrand, Coupling of fast multipole method and microlocal discretization for the 3-D Helmholtz equation, *Journal of Computational Physics* 181 (2002) 126–154.
[40] E. Perrey-Debain, J. Trevelyan, P. Bettess, Plane wave interpolation in direct collocation boundary element method for radiation and wave scattering: numerical aspects and applications, *Journal of Sound and Vibration* 261 (2003) 839–858.
[41] S.N. Chandler-Wilde, S. Langdon, L. Ritter, A high-wavenumber boundary-element method for an acoustics scattering problem, *Philosophical Transactions of Royal Society of London* 362 (2004) 647–671.
[42] S. Järvenpää, M. Taskinen, P. Ylä-Oijala, Singularity extraction technique for integral equation methods with high order basis functions on plane triangles and tetrahedra, *International Journal for Numerical Methods in Engineering* 58 (2003) 1149–1165.
[43] A. Sihvola, P. Ylä-Oijala, S. Järvenpää, J. Avelin, Polarizabilities of Platonic solids, *IEEE Transactions on Antennas and Propagation* 52 (9) (2004) 2226–2233.
[44] Y. Saad, *Iterative Methods for Sparse Linear Systems*, PWS Publishing, New York, 1996.
[45] K. Sertel, J.L. Volakis, Incomplete LU preconditioner for FMM implementation, *Microwave and Optical Technology Letters* 26 (4) (2000) 265–267.
[46] J. Lee, J. Zhang, C-C. Lu, Incomplete LU preconditioner for large scale dense complex linear systems from electromagnetic wave scattering problems, *Journal of Computational Physics* 185 (1) (2003) 158–175.
[47] R. Kress, Minimizing the condition number of boundary integral operators in acoustic and electromagnetic scattering, *The Quarterly Journal of Mechanics and Applied Mathematics* 38 (2) (1985) 323–341.
[48] S. Amini, On the choice of coupling parameter in boundary integral formulations of the acoustic problem, *Applied Analysis* 35 (1990) 75–92.
[49] P. Geng, J.T. Oden, L. Demkowicz, Numerical solution and a posteriori error estimation of exterior acoustics problems by a boundary element method at high wave numbers, *Journal of Acoustic Society of America* 100 (1) (1996) 335–345.

[50] H. Kardestuncer (Editor-in-Chief), D.H. Norrie (Project Editor), *Finite Element Handbook*, McGraw-Hill, New York, 1987.
[51] P. Ylä-Oijala, M. Taskinen, Calculation of CFIE impedance matrix elements with RWG and $\mathbf{n}\times$ RWG functions, *IEEE Transactions of Antennas and Propagation* 51 (2003) 1837–1846.
[52] S.A. Yang, An investigation into integral equation methods involving nearly singular kernels for acoustic scattering, *Journal of Sound and Vibration* 234 (2) (2000) 225–239.
[53] D.R. Wilton, M.A. Khayat, Evaluation of singular and near-singular potential integrals, in: *Proceedings of 2003 USNC/CNC/URSI North American Radio Science Meeting*, June 22–27, 2003, Columbus, Ohio, USA, p. 394.
[54] S. Caorsi, D. Moreno, F. Sidoti, Theoretical and numerical treatment of surface integrals involving the free-space Green's function, *IEEE Transaction on Antennas and Propagation* 41 (1993) 1296–1301.
[55] S.A. Yang, Acoustic scattering by a hard or soft body across a wide frequency range by the Helmholtz integral equation method, *Journal of Acoustic Society of America* 102 (5) (1997) 2511–2520.
[56] R. Barrett, M.W. Berry, T.F. Chan, J. Demmel, J. Donato, J. Dongarra, V. Eijkhout, R. Pozo, C. Romine, H. van der Vorst, *Templates for the Solution of Linear Systems: Building Blocks for Iterative Methods*, SIAM, Philadelphia, PA, 1994.
[57] S.W. Sloan, An algorithm for profile and wavefront reduction of sparse matrices, *International Journal for Numerical Methods in Engineering* 23 (1986) 239–251.
[58] S.W. Sloan, A Fortran program for profile and wavefront reduction, *International Journal for Numerical Methods in Engineering* 28 (1989) 2651–2679.
[59] S.N. Makarov, M. Ochmann, An iterative solver of the Helmholtz integral equation for high-frequency acoustic scattering, *Journal of Acoustic Society of America* 103 (2) (1998) 742–750.
[60] J.-S. Zhao, W.C. Chew, Integral equation solution of Maxwell's equations from zero frequency to microwave frequencies, *IEEE Transactions of Antennas and Propagation* 48 (10) (2000) 1635–1645.